

Performance Analysis of Approximate Message Passing for Distributed Compressed Sensing

Gabor Hannak, Alessandro Perelli, Norbert Goertz, *Senior Member, IEEE*, Gerald Matz, *Senior Member, IEEE*, and Mike E. Davies, *Fellow, IEEE*

Abstract—Bayesian approximate message passing (BAMP) is an efficient method in compressed sensing that is nearly optimal in the minimum mean squared error (MMSE) sense. Bayesian approximate message passing (BAMP) performs joint recovery of multiple vectors with identical support and accounts for correlations in the signal of interest and in the noise. In this paper, we show how to reduce the complexity of vector BAMP via a simple joint decorrelation (diagonalization) transform of the signal and noise vectors, which also facilitates the subsequent performance analysis. We prove that BAMP and the corresponding state evolution (SE) are equivariant with respect to the joint decorrelation transform and preserve diagonality of the residual noise covariance for the Bernoulli-Gauss (BG) prior. We use these results to analyze the dynamics and the mean squared error (MSE) performance of BAMP via the replica method, and thereby understand the impact of signal correlation and number of jointly sparse signals.

I. INTRODUCTION

Compressed sensing (CS) is a signal processing technique aiming at recovering a high-dimensional sparse vector from a (noisy) system of linear equations [1], [2]. Joint sparsity refers to multiple vectors having the same support set¹, whose cardinality is typically much lower than the signal dimension. There are two prominent CS scenarios [3], [4]: (i) the multiple measurement vector (MMV) problem, where the measurement matrices are identical, and (ii) the distributed compressed sensing (DCS) problem, where the measurement matrices are independent. Joint sparsity arises in a number of real-world scenarios which multiple sensors or antennas observe the same signal corrupted by different channels and noise signals (e.g., [3], [4]). Typical applications are magnetic resonance imaging [5], distributed networks [6], wireless communications [7], and direction of arrival estimation [8].

A. Related Work

Several methods for jointly sparse recovery have been proposed in the literature [3], [6], [9]–[18]. Approximate message passing (AMP) was introduced in [19]–[21] as a large system relaxation of loopy belief propagation to solve a random linear

G. Hannak, N. Goertz, and G. Matz are with the Institute of Telecommunications, Vienna University of Technology, Vienna, Austria (e-mail: ghannak@nt.tuwien.ac.at, ngoertz@nt.tuwien.ac.at, gmatz@nt.tuwien.ac.at)

A. Perelli and M. E. Davies are with the Institute of Digital Communications, University of Edinburgh, Edinburgh, UK, (e-mail: m.davies@ed.ac.uk; a.perelli@ed.ac.uk)

This work was funded in part by WWTF Grant ICT15-119, ERC Grant 694888, and EPSRC Grant EP/M008916/1.

¹The support set of a vector comprises the indices of the vector's nonzero entries.

system with sparsity constraint. Scalar Bayesian approximate message passing (BAMP), its Bayesian version [22], [23], uses the signal prior explicitly and is an efficient approximate MMSE estimator. The turbo BAMP methods in [13]–[15] improve the recovery performance by exchanging extrinsic information about the current support estimate in each message passing iteration. In [16], [17], [24], joint sparsity is directly enforced by an appropriate vector estimator (denoiser) function for the Bernoulli-Gauss (BG) prior. The state evolution (SE) formalism developed in [20], [21], [25] analytically predicts the recovery performance of (B)AMP algorithms. SE was employed to analyze BAMP for joint sparsity with a vector estimator and to point out the difference between the DCS and MMV scenarios in [17]. In [24], the replica method (a non-rigorous statistical physics tool for large disordered systems) is used to calculate the MMSE of the CS measurement (note that [24] refers to MMV and DCS as MMV-2 and MMV-1, respectively). The replica trick specifically simplifies the high-dimensional integral for the MMSE of the Bayesian estimator of the CS channel, thereby leading to the free energy as a function of the mean squared error (MSE). The local maxima in the free energy function correspond to fixed points of belief propagation (BP) and BAMP and thus predict the expected MSE of BAMP. The replica analysis in [24] is performed for the BG signal prior with uncorrelated isotropic unitary signal and uncorrelated isotropic noise distribution (i.e., with a single noise parameter).

B. Contributions

We consider the vector Bayesian approximate message passing (BAMP) algorithm for the DCS and MMV problems, which uses an appropriate vector MMSE estimator function and Onsager correction term to exploit joint sparsity structure, the signal distribution, and the noise covariance. We provide an analytical performance prediction for the BAMP algorithm with BG signal prior with arbitrary signal and noise correlation by (i) incorporating a linear joint decorrelation of the measurements, (ii) showing the equivariance of BAMP w.r.t. invertible linear transformations, (iii) extending the replica analysis from [24] to arbitrary diagonal noise covariance matrices.

In particular, the joint decorrelation yields a simpler equivalent measurement model with diagonal signal and noise covariance matrix (under mild conditions, one of the covariance matrices can be made the identity matrix). The simplified model naturally provides the measurement signal-to-noise ratios (SNRs) of each signal vector and substantially

reduces the complexity of the BAMP iterations. We further show that the BAMP algorithm is equivariant to invertible linear transformations, thus, it preserves its properties across iterations in the transformed domain and delivers a result equivalent to that obtained with the original measurements. For the widely used BG prior, we prove that the BAMP iterations (and the corresponding SE) preserve the diagonal structure of the (effective) noise covariance, thus implying that a B -dimensional state (instead of $B(B+1)/2$ dimensions) is sufficient and that every MMV problem can be transformed into an equivalent DCS problem. Finally, we extend the replica analysis in [24] to the case of anisotropic noise (i.e., B noise parameters instead of just 1). The replica analysis yields the B measurement-wise MSEs of the BAMP estimate in its stationary points.

C. Outline

The remainder of this paper is organized as follows. In Section II, we discuss the BAMP algorithm, the estimator function for the multivariate BG signal prior, and the multivariate state evolution of BAMP. In Section III, the joint decorrelation of the signal and the noise vectors is investigated in the context of BAMP and state evolution; the multivariate BG signal prior is studied as special case. In Section IV, we present the multivariate free energy formula for arbitrary diagonal noise covariance matrices (the details of the replica analysis are relegated to the appendix). Section V provides a qualitative discussion and open questions regarding the effects of signal correlation and the increasing number of jointly sparse vectors on the dynamics of BAMP. We close with conclusions in Section VI.

D. Notation

Uppercase (lowercase) boldface letters denote matrices (vectors), and serif letters denote random quantities. For a matrix \mathbf{A} (vector \mathbf{a}), \mathbf{A}_i (a_i) denotes its i th row (i th entry). The all zero matrix and the identity matrix of dimension $M \times N$ are denoted by $\mathbf{0}_{M \times N}$ and $\mathbf{I}_{M \times N}$, respectively (we omit the subscript if the dimensions are clear from the context). The Dirac delta (generalized) function is $\delta(\mathbf{x})$. The normal distribution with mean $\boldsymbol{\mu}$ and covariance matrix $\boldsymbol{\Sigma}$ is denoted by $\mathcal{N}(\boldsymbol{\mu}, \boldsymbol{\Sigma})$ and $\mathcal{N}(\mathbf{x}; \boldsymbol{\mu}, \boldsymbol{\Sigma})$ denotes the value of this normal probability density function (pdf) at \mathbf{x} . The outer product of a column vector \mathbf{x} with itself is denoted by $\langle \mathbf{x} \rangle = \mathbf{x}\mathbf{x}^T$. For a vector $\mathbf{x} = (x_1, \dots, x_B)^T$, $\text{diag}(\mathbf{x})$ and $\text{diag}(x_1, \dots, x_B)$ is the diagonal matrix whose i th diagonal element equals x_i . For a matrix \mathbf{X} , $D(\mathbf{X})$ is the diagonal matrix whose diagonal is identical to that of \mathbf{X} , i.e., $D(\cdot)$ is the orthogonal projection that zeros the off-diagonal elements. The Kronecker product of two matrices is denoted by \otimes .

II. BAMP WITH VECTOR DENOISER

A. Measurement Model

We consider the measurement model

$$\mathbf{y}(b) = \mathbf{A}(b)\mathbf{x}(b) + \mathbf{w}(b), \quad (1)$$

Algorithm 1 BAMP for MMV/DCS

```

1: input:  $\mathbf{y}(b)$ ,  $\mathbf{A}(b)$ ,  $\boldsymbol{\Sigma}_{\bar{\mathbf{x}}}$ 
2:  $t = 0$ ,  $\bar{\mathbf{x}}_n^t = \mathbf{0}_{B \times 1}$ ,  $\bar{\mathbf{r}}_m^t = \bar{\mathbf{y}}_m$ ,  $\forall m, n$ 
3: do
4:    $t \leftarrow t + 1$ 
5:    $\mathbf{u}^{t-1}(b) = \hat{\mathbf{x}}^{t-1}(b) + \mathbf{A}(b)^T \mathbf{r}^{t-1}(b) \forall b$ 
6:    $\boldsymbol{\Sigma}_{\bar{\mathbf{v}}}^{t-1} = \begin{cases} \text{Cov}\{\bar{\mathbf{r}}_m^{t-1}\} & \text{for MMV} \\ D(\text{Cov}\{\bar{\mathbf{r}}_m^{t-1}\}) & \text{for DCS} \end{cases}$ 
7:    $\hat{\bar{\mathbf{x}}}_n^t = F(\bar{\mathbf{u}}_n^{t-1}; \boldsymbol{\Sigma}_{\bar{\mathbf{v}}}^{t-1}) \forall n$ 
8:    $\bar{\mathbf{r}}_m^t = \bar{\mathbf{y}}_m - (\mathbf{A}(1)\hat{\bar{\mathbf{x}}}_1^t, \dots, \mathbf{A}(B)\hat{\bar{\mathbf{x}}}_B^t)_m$ 
    $+ \frac{1}{M} \sum_{n=1}^M F'(\bar{\mathbf{u}}_n^{t-1}; \boldsymbol{\Sigma}_{\bar{\mathbf{v}}}^{t-1}) \bar{\mathbf{r}}_m^t \forall m$ 
9:   while  $\sum_{b=1}^B \|\hat{\mathbf{x}}^t(b) - \hat{\mathbf{x}}^{t-1}(b)\|_2^2 > \epsilon_{\text{tol}} \sum_{b=1}^B \|\hat{\mathbf{x}}^{t-1}(b)\|_2^2$ 
   and  $t < t_{\text{max}}$ 
10: return  $\hat{\mathbf{x}}(b) = \hat{\mathbf{x}}^t(b)$ ,  $\forall b$ 

```

with $\mathbf{y}(b) \in \mathbb{R}^M$, $\mathbf{x}(b) \in \mathbb{R}^N$, $\mathbf{w}(b) \in \mathbb{R}^M$, and $\mathbf{A}(b) \in \mathbb{R}^{M \times N}$, for $b = 1, \dots, B$. We denote the measurement rate by $R = M/N$. We assume that the measurement matrices $\mathbf{A}(b)$ are realizations of Gaussian or Rademacher random matrices [26] with normalized columns. If the measurement matrices $\mathbf{A}(b)$ are identical (i.e., $\mathbf{A}(b) = \mathbf{A}$, $b = 1, \dots, B$) we have an MMV scenario; if they are mutually independent then we have a DCS scenario. We define the length- B column vectors

$$\begin{aligned} \bar{\mathbf{x}}_n &= (x_n(1), \dots, x_n(B))^T, \\ \bar{\mathbf{y}}_m &= (y_m(1), \dots, y_m(B))^T, \\ \bar{\mathbf{w}}_m &= (w_m(1), \dots, w_m(B))^T \end{aligned}$$

(similar notation will be used throughout the paper). Joint sparsity (cf. JSM-2 in [4]) with sparsity (or nonzero probability) ϵ requires that $\bar{\mathbf{x}}_n = \mathbf{0}$ with probability $1 - \epsilon$ and $\bar{\mathbf{x}}_n \neq \mathbf{0}$ with probability ϵ . In this work, we focus on signals with multivariate BG pdf, i.e.,

$$f_{\bar{\mathbf{x}}_n}(\bar{\mathbf{x}}_n) = \bar{f}_{\bar{\mathbf{x}}_n}(\bar{\mathbf{x}}_n) = (1 - \epsilon) \delta(\bar{\mathbf{x}}_n) + \epsilon \mathcal{N}(\bar{\mathbf{x}}_n; \mathbf{0}, \boldsymbol{\Sigma}_{\bar{\mathbf{x}}}), \quad (2)$$

independent and identically distributed (i.i.d.) over n ; here, $\boldsymbol{\Sigma}_{\bar{\mathbf{x}}}$ is the covariance matrix of $\bar{\mathbf{x}}_n$ given that it is non-zero vector. The additive noise in (1) is assumed to be i.i.d. Gaussian over m with zero mean and covariance $\boldsymbol{\Sigma}_{\bar{\mathbf{w}}}$,

$$\bar{\mathbf{w}}_m \sim \mathcal{N}(\mathbf{0}, \boldsymbol{\Sigma}_{\bar{\mathbf{w}}}).$$

B. Vector BAMP for MMV/DCS

The BAMP method for joint sparse recovery of $\mathbf{x}(b)$, $b = 1, \dots, B$, [16], [18] is summarized in Algorithm 1 (superscript t indicates the iteration index). Note that scalar BAMP (i.e., when $B = 1$) is a special case of Algorithm 1 where MMV and DCS are equivalent. It follows similar steps as ordinary scalar BAMP [19]–[23], [25]. According to the decoupling principle [23], which holds in the asymptotic regime where $M, N \rightarrow \infty$ while $\frac{M}{N} = R$, the BAMP algorithm decouples the CS measurements (1) according to

$$\bar{\mathbf{u}}_n^t = \bar{\mathbf{x}}_n + \bar{\mathbf{v}}_n^t,$$

where the effective noise vector is distributed as $\bar{\mathbf{v}}_n^t \sim \mathcal{N}(\mathbf{0}, \boldsymbol{\Sigma}_{\bar{\mathbf{v}}}^t)$. The effective noise covariance is estimated

via the empirical covariance in line 6. It has been shown in [17] that in the DCS scenario only the diagonal entries of the covariance matrix are retained due to the mixing effected by the B independent measurement matrices. In the following, we will simplify notation by occasionally dropping the indices t and n .

The vector denoiser in BAMP (line 7 of Algorithm 1) amounts to a vector MMSE estimator of \vec{x}_n given the decoupled measurements \vec{u}_n . Using Bayes' theorem, the denoiser can be written as:

$$F(\vec{u}; \Sigma_{\vec{v}}) = E_{\vec{x}} \{ \vec{x} \mid \vec{u} = \vec{u}; \Sigma_{\vec{v}} \} \\ = \frac{\int_{\mathbb{R}^B} \vec{z} \mathcal{N}(\vec{u}; \vec{z}, \Sigma_{\vec{v}}) f_{\vec{x}}(\vec{z}) d\vec{z}}{\int_{\mathbb{R}^B} \mathcal{N}(\vec{u}; \vec{z}, \Sigma_{\vec{v}}) f_{\vec{x}}(\vec{z}) d\vec{z}}, \quad (3)$$

where the covariance of the effective noise is $\Sigma_{\vec{v}} = \text{Cov}\{\vec{r}\}$ (MMV) or $\Sigma_{\vec{v}} = D(\text{Cov}\{\vec{r}\})$ (DCS). For the multivariate BG prior (2), the vector denoiser becomes

$$F(\vec{u}; \Sigma_{\vec{v}}) = \mathbf{W} \vec{u} \quad \text{with} \quad \mathbf{W} = \frac{F_N(\vec{u}; \Sigma_{\vec{v}})}{F_D(\vec{u}; \Sigma_{\vec{v}})} \Sigma_{\vec{x}} \Sigma_{\vec{u}}^{-1}. \quad (4)$$

Here, $\Sigma_{\vec{u}} = \Sigma_{\vec{x}} + \Sigma_{\vec{v}}$ and

$$F_N(\vec{u}; \Sigma_{\vec{v}}) = \epsilon \mathcal{N}(\vec{u}; \mathbf{0}, \Sigma_{\vec{u}}), \\ F_D(\vec{u}; \Sigma_{\vec{v}}) = (1 - \epsilon) \mathcal{N}(\vec{u}; \mathbf{0}, \Sigma_{\vec{v}}) + \epsilon \mathcal{N}(\vec{u}; \mathbf{0}, \Sigma_{\vec{u}}).$$

The denoiser (4) consists of a multivariate Gaussian Wiener estimator followed by a joint shrinkage operation.

The BAMP residual is computed in line 8 of Algorithm 1. As in the original AMP derivation [22], the Onsager correction term for the residual $\vec{y}_m - (\mathbf{A}(1)\hat{\mathbf{x}}(1), \dots, \mathbf{A}(B)\hat{\mathbf{x}}(B))_m$ is computed via the derivative of the estimator. In the asymptotic regime, the Onsager term

$$\frac{1}{M} \sum_{n=1}^N F'(\vec{u}_n; \Sigma_{\vec{v}}) \vec{r}_m \quad (5)$$

renders the decoupled measurement vectors \vec{u}_n Gaussian with mean \vec{x}_n and covariance $\Sigma_{\vec{v}}$ [18], [24]. Here, the Jacobian matrix $F'(\vec{u}; \Sigma_{\vec{v}}) = dF(\vec{u}; \Sigma_{\vec{v}})/d\vec{u}^T$ of the estimator $F(\vec{u}; \Sigma_{\vec{v}})$ is given by

$$F'(\vec{u}; \Sigma_{\vec{v}}) = \mathbf{W} - \left(1 - \frac{F_N(\vec{u}; \Sigma_{\vec{v}})}{F_D(\vec{u}; \Sigma_{\vec{v}})} \right) \mathbf{W} \vec{u}_n \vec{u}_n^T (\Sigma_{\vec{u}}^{-1} - \Sigma_{\vec{w}}^{-1}).$$

The algorithm runs until the relative change in the estimated signal is below a certain threshold ϵ_{tol} or the maximum number of iterations t_{max} is reached. Compared to scalar BAMP, the vector BAMP algorithm involves the following crucial modifications:

- a multivariate prior (possibly with joint sparsity structure and correlation);
- the estimator acts on vectors rather than scalars (3) and both correlated signal and correlated additive noise are taken into consideration (more precisely, the full signal and noise vector pdf is taken into account);
- an Onsager term obtained as the sum of Jacobian matrices (cf. (5)).

Algorithm 2 joint diagonalization transformation

- 1: Given $\Sigma_{\vec{x}}, \Sigma_{\vec{w}}$
 - 2: find \mathbf{P} such that $\mathbf{P}\mathbf{P}^T = \Sigma_{\vec{w}}$
 - 3: $\mathbf{G} = \mathbf{P}^{-1}\Sigma_{\vec{x}}\mathbf{P}^{-T}$
 - 4: find eigendecomposition $\mathbf{Q}\mathbf{\Lambda}\mathbf{Q}^T = \mathbf{G}$
 - 5: $\mathbf{T} = \mathbf{\Lambda}^{-1/2}\mathbf{Q}^T\mathbf{P}^{-1}$
-

C. State Evolution

SE was originally proposed in [19] for scalar (B)AMP and extended to the MMV and DCS scenarios e.g. in [17]; it allows to characterize analytically the expected behavior of BAMP (note that the Onsager term in [17] is flawed even though the multivariate SE is correct). In particular, the SE equation predicts the evolution of the effective noise covariance (the state) for any signal prior $\vec{x} \sim g_{\vec{x}}(\vec{x}_n)$ as

$$\Sigma_{\vec{v}}^{t+1} = \begin{cases} \Sigma_{\vec{w}} + \frac{1}{R} E_{\vec{x}, \vec{v}} \{ \langle \mathbf{e}(\vec{x}, \vec{v}) \rangle \} & \text{for MMV,} \\ D(\Sigma_{\vec{w}} + \frac{1}{R} E_{\vec{x}, \vec{v}} \{ \langle \mathbf{e}(\vec{x}, \vec{v}) \rangle \}) & \text{for DCS,} \end{cases} \quad (6)$$

where $\mathbf{e}(\vec{x}, \vec{v}) = F(\vec{x} + \vec{v}; \Sigma_{\vec{v}}^t) - \vec{x}$ is the error achieved by the MMSE estimator $F(\vec{u}; \Sigma_{\vec{v}}^t)$ and $\vec{v} \sim \mathcal{N}(\mathbf{0}, \Sigma_{\vec{v}}^t)$. The state in the MMV scenario is in general $B(B+1)/2$ dimensional (since the covariance matrix is symmetric). From (6), the MSE prediction directly follows as

$$\text{Cov}\{\vec{u}_n^t - \vec{x}_n\} = \Sigma_{\vec{v}}^t, \\ \widehat{\text{MSE}}^t(b) = R(\Sigma_{\vec{v}}^t - \Sigma_{\vec{w}})_{b,b},$$

with the MSE per channel being defined as

$$\text{MSE}^t(b) = \frac{1}{N} \|\hat{\mathbf{x}}^t(b) - \mathbf{x}(b)\|_2^2.$$

III. DIAGONALIZED VECTOR BAMP

A. Joint Diagonalization for MMV

The BAMP algorithm in Section II-B can deal with arbitrary signal and noise correlations $\Sigma_{\vec{x}}$ and $\Sigma_{\vec{w}}$, which in general results in a nondiagonal $\Sigma_{\vec{v}}^t$ in the MMV scenario. In the decoupled measurements $\vec{u} = \vec{x} + \vec{v}$, it means that there are $\mathcal{O}(B^2)$ SNR relations and $B(B+1)/2$ states: each $x_n(b)$ correlates with all $x_n(b')$, $b' \in \{1, \dots, B\} \setminus \{b\}$, and it is influenced simultaneously by all effective noise components $v(b')$, $b' \in \{1, \dots, B\}$.

Under the assumption that the covariance matrices $\Sigma_{\vec{x}}$ and $\Sigma_{\vec{w}}$ are full rank and using the fact that covariance matrices are symmetric and positive definite and [27, Thm. 7.6.1.], there exists a nonsingular (but generally non-orthogonal) matrix \mathbf{T} that simultaneously diagonalizes the covariance matrices of the signal \vec{x} and the noise \vec{w} . The computation of \mathbf{T} is described in Algorithm 2. In the transformed model

$$\tilde{\vec{y}}_m = \mathbf{T}\vec{y}_m, \quad \tilde{\vec{x}}_n = \mathbf{T}\vec{x}_n, \quad \tilde{\vec{w}}_m = \mathbf{T}\vec{w}_m, \quad (7)$$

we thus have

$$\Sigma_{\tilde{\vec{x}}} = \mathbf{T}\Sigma_{\vec{x}}\mathbf{T}^T = \mathbf{I}_{B \times B}, \\ \Sigma_{\tilde{\vec{w}}} = \mathbf{T}\Sigma_{\vec{w}}\mathbf{T}^T = \mathbf{\Lambda}^{-1} = \epsilon \text{diag} \left(\frac{1}{\text{SNR}(1)}, \dots, \frac{1}{\text{SNR}(B)} \right).$$

Here, the per-channel SNRs are defined as

$$\text{SNR}(b) = \frac{\mathbb{E}_{\mathbf{x}}\{\|\mathbf{A}(b)\tilde{\mathbf{x}}(b)\|_2^2\}}{\mathbb{E}_{\mathbf{w}}\{\|\tilde{\mathbf{w}}(b)\|_2^2\}} = \epsilon \boldsymbol{\Lambda}_{b,b}.$$

Note that the decorrelation can be applied also in the DCS scenario, given that only the noise covariance $\boldsymbol{\Sigma}_{\tilde{\mathbf{w}}}$ is nondiagonal and the signal covariance $\boldsymbol{\Sigma}_{\tilde{\mathbf{x}}}$ is diagonal. We emphasize that in case BAMP operates on the transformed measurements, the change in the prior distribution has to be accounted for in a nontrivial manner. That is, the MMSE estimator (3) and its derivative will have a different form. Consider the SE equation (6) that describes the expected evolution of the effective noise covariance over the BAMP iterations. In the MMV scenario, even if $\boldsymbol{\Sigma}_{\tilde{\mathbf{w}}}$ and $\boldsymbol{\Sigma}_{\tilde{\mathbf{v}}}^t$ are diagonal, $\boldsymbol{\Sigma}_{\tilde{\mathbf{v}}}^{t+1}$ in general will not be diagonal because the estimator $F(\tilde{\mathbf{u}}_n^t, \hat{\boldsymbol{\Sigma}}_{\tilde{\mathbf{v}}}^t)$ operates on the overall vector $\tilde{\mathbf{u}}_n^t$ (the diagonalization described in Algorithm 2 could be performed repeatedly in each iteration). However, we will see shortly that in the particular case of the BG prior this is no longer the case. A direct calculation reveals that

$$\text{Cov}\{\tilde{\mathbf{y}}_m\} = \begin{cases} \boldsymbol{\Sigma}_{\tilde{\mathbf{w}}} + \frac{1}{R} \text{Cov}\{\tilde{\mathbf{x}}_n\} & \text{for MMV,} \\ \boldsymbol{\Sigma}_{\tilde{\mathbf{w}}} + \frac{1}{R} D(\text{Cov}\{\tilde{\mathbf{x}}_n\}) & \text{for DCS.} \end{cases}$$

Thus, when estimating the signal/noise parameters via the empirical covariance $\text{Cov}\{\tilde{\mathbf{y}}_m\}$, either the noise or the signal covariance has to be known a priori. We refer the interested reader to the expectation-maximization AMP approach introduced in [28], which could be applied to estimate the unknown parameters during iterations when the measured signal comes from a (Bernoulli-)Gaussian mixture.

B. Equivariance of BAMP for MMV

We next establish the fact that for MMV both BAMP and its SE are equivariant w.r.t. invertible linear transformations of the input. The proof of this result is provided in Appendix A.

Theorem 1: Algorithm 1 for MMV and its SE are equivariant w.r.t. invertible linear transformations. Denote one BAMP iteration by $(\hat{\tilde{\mathbf{x}}}_n^{t+1}, \hat{\tilde{\mathbf{r}}}_m^{t+1}, \hat{\boldsymbol{\Sigma}}_{\tilde{\mathbf{v}}}^{t+1}) = \mathbf{V}(\tilde{\mathbf{y}}_m, \hat{\tilde{\mathbf{x}}}_n^t, \hat{\tilde{\mathbf{r}}}_m^t, \hat{\boldsymbol{\Sigma}}_{\tilde{\mathbf{v}}}^t)$. For any nonsingular \mathbf{T} , we have for all m and n

$$\mathbf{V}(\mathbf{T}\tilde{\mathbf{y}}_m, \mathbf{T}\hat{\tilde{\mathbf{x}}}_n^t, \mathbf{T}\hat{\tilde{\mathbf{r}}}_m^t, \mathbf{T}\hat{\boldsymbol{\Sigma}}_{\tilde{\mathbf{v}}}^t) = (\mathbf{T}\hat{\tilde{\mathbf{x}}}_n^{t+1}, \mathbf{T}\hat{\tilde{\mathbf{r}}}_m^{t+1}, \mathbf{T}\hat{\boldsymbol{\Sigma}}_{\tilde{\mathbf{v}}}^{t+1}\mathbf{T}^T).$$

Furthermore, the SE equation (6) translates to the transformed domain as

$$\mathbf{T}\boldsymbol{\Sigma}_{\tilde{\mathbf{v}}}^{t+1}\mathbf{T}^T = \mathbf{T}\boldsymbol{\Sigma}_{\tilde{\mathbf{w}}}\mathbf{T}^T + \frac{1}{R} \mathbb{E}_{\tilde{\mathbf{x}}, \tilde{\mathbf{v}}}\{ \langle F(\mathbf{T}(\tilde{\mathbf{x}} + \tilde{\mathbf{v}}); \mathbf{T}\boldsymbol{\Sigma}_{\tilde{\mathbf{v}}}^t\mathbf{T}^T) - \mathbf{T}\tilde{\mathbf{x}} \rangle \}. \quad (8)$$

Note that (8) holds for any signal prior in the Bayesian setting, i.e., when the estimator is the MMSE estimator. Assume that BAMP converges to $\hat{\tilde{\mathbf{x}}}_n$ with inputs $\tilde{\mathbf{y}}_n$, $\boldsymbol{\Sigma}_{\tilde{\mathbf{x}}}$, and $\boldsymbol{\Sigma}_{\tilde{\mathbf{w}}}$; then, Theorem 1 implies that BAMP with inputs $\mathbf{T}\tilde{\mathbf{y}}_n$, $\mathbf{T}\boldsymbol{\Sigma}_{\tilde{\mathbf{x}}}\mathbf{T}$, and $\mathbf{T}\boldsymbol{\Sigma}_{\tilde{\mathbf{w}}}\mathbf{T}$ converges to the solution $\mathbf{T}\hat{\tilde{\mathbf{x}}}_n$.

C. Bernoulli-Gauss Prior

For the BG prior, after applying the transformation \mathbf{T} , the equivalent measurement model becomes

$$\tilde{\mathbf{y}}(b) = \mathbf{A}(b)\tilde{\mathbf{x}}(b) + \tilde{\mathbf{w}}(b), \quad \forall b \quad (9)$$

with signal and noise pdfs

$$f_{\tilde{\mathbf{x}}}(\tilde{\mathbf{x}}_n) = (1 - \epsilon) \delta(\tilde{\mathbf{x}}_n) + \epsilon \mathcal{N}(\tilde{\mathbf{x}}_n; \mathbf{0}, \mathbf{I}), \quad (10)$$

$$f_{\tilde{\mathbf{w}}}(\tilde{\mathbf{w}}_m) = \mathcal{N}(\tilde{\mathbf{w}}_m; \mathbf{0}, \boldsymbol{\Lambda}^{-1}). \quad (11)$$

That is, we retain a BG prior in the transformed domain, only with uncorrelated components. This is a distinctive feature of the BG prior and in general doesn't hold for other types of distributions.

In Appendix B we demonstrate that for the decorrelated model (9) with BG prior (10)–(11), the BAMP iterations under the MMV model preserve the diagonal structure of $\boldsymbol{\Sigma}_{\tilde{\mathbf{v}}}^t$. It follows that for CS measurements with multivariate BG signal prior, the decorrelation transformation has to be done only once before recovery; determining \mathbf{T} itself is of negligible computational effort unless B is very large. These observations have the following implications:

- The computation of (4) and (5) is significantly simplified, leading to complexity reductions by a factor of B .
- The dimension of the SE equations is B instead of $B(B+1)/2$. In other words, $B(B+1)/2$ effective noise covariance parameters in $\boldsymbol{\Sigma}_{\tilde{\mathbf{v}}}$ are reduced to B effective noise variances, which explicitly characterize the MSE for each signal vector estimate as

$$\widehat{\text{MSE}}^t(b) = R(\boldsymbol{\Sigma}_{\tilde{\mathbf{v}}}^t - \boldsymbol{\Sigma}_{\tilde{\mathbf{w}}})_{b,b}.$$

- Every MMV problem has an equivalent DCS problem with possibly rescaled SNRs. Furthermore, the analysis of DCS also covers that of MMV.

IV. REPLICANALYSIS

In [24], the replica method was used to determine the MSE performance of BAMP for the measurement (1) and the BG prior (2), assuming $\boldsymbol{\Sigma}_{\tilde{\mathbf{x}}} = \mathbf{I}$ and isotropic uncorrelated noise, i.e., $\boldsymbol{\Sigma}_{\tilde{\mathbf{w}}} = \sigma_w^2 \mathbf{I}$. In this special case MMV and DCS (referred to as MMV-2 and MMV-1, respectively, in [24]) are equivalent. The analysis is quite sophisticated and the generalization to arbitrary signal and noise correlations seems infeasible. However, due to the joint diagonalization approach from Section III, it suffices to extend the replica analysis to the case with $\boldsymbol{\Sigma}_{\tilde{\mathbf{x}}} = \mathbf{I}$ and $\boldsymbol{\Sigma}_{\tilde{\mathbf{w}}} = \text{diag}(\sigma_w^2(1), \dots, \sigma_w^2(B))$. In particular, the replica method is capable of predicting the fixed points of BAMP in the asymptotic regime ($N, M \rightarrow \infty$, $R = M/N = \text{const.}$), as a function of the set of B MSEs [29], [30]. We note that rigorous equivalence between the replica method and SE is not always guaranteed and requires additional technicalities [31]. Assuming $\boldsymbol{\Sigma}_{\tilde{\mathbf{x}}} = \mathbf{I}$ and $\boldsymbol{\Sigma}_{\tilde{\mathbf{w}}} = \text{diag}(\sigma_w^2(1), \dots, \sigma_w^2(B))$, we compute in Appendix

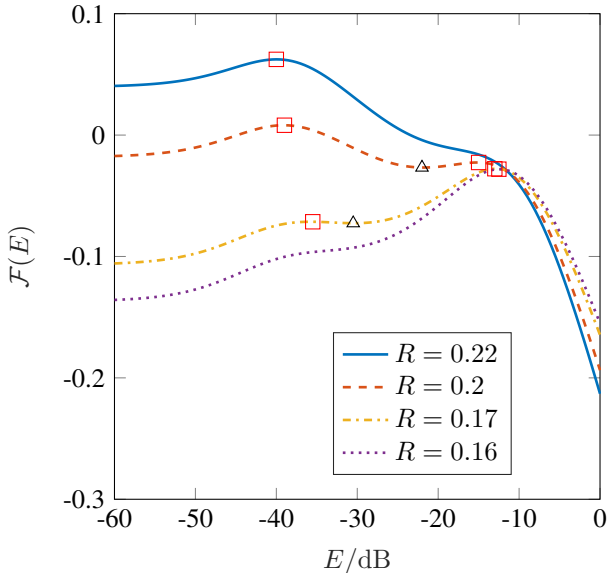


Figure 1: Free energy function at different rates R for the isotropic case with $\sigma_w^2 = -35$ dB and sparsity $\epsilon = 0.1$. Red squares and black triangles indicate local maxima and minima, respectively.

C the free energy $\mathcal{F}(\vec{\mathbf{E}})$ as a function of the MSE vector $\vec{\mathbf{E}} = (E(1), \dots, E(b))^T$ with $E(b) = \text{MSE}(b)$, resulting in

$$\mathcal{F}(\vec{\mathbf{E}}) = (1 - \epsilon)\zeta(\gamma) + \epsilon\zeta\left(\frac{\gamma}{1 + \gamma}\right) - \frac{R}{2} \sum_{b=1}^B \left(\log \frac{2\pi R}{\gamma(b)} + \gamma(b)\sigma_w^2(b) - \frac{1 - \epsilon}{R} \frac{\gamma(b)}{1 + \gamma(b)} \right). \quad (12)$$

In this expression we used

$$\zeta(\eta) = \int \log \left(\epsilon \prod_{b=1}^B (1 + \gamma(b))^{-\frac{1}{2}} + (1 - \epsilon) \exp \left(-\frac{1}{2} \sum_{b=1}^B \eta(b) h^2(b) \right) \right) \mathcal{D}\mathbf{h}$$

with

$$\gamma(b) = \frac{R}{E(b) + R\sigma_w^2(b)};$$

furthermore, $\mathcal{D}\mathbf{h} = \mathcal{N}(\mathbf{h}; \mathbf{0}, \mathbf{I}) dh_1 \dots dh_B$ denotes the multivariate standard Gaussian measure.

The stationary points of $\mathcal{F}(\vec{\mathbf{E}})$ correspond to fixed points of belief propagation [32], and hence to those of BAMP in the asymptotic regime [24]. Thus, we can determine the component-wise MSEs of BAMP by evaluating (12) and finding the largest components of $\vec{\mathbf{E}}$ that correspond to a local maximum of $\mathcal{F}(\vec{\mathbf{E}})$ [33], [34]. Note that for isotropic noise ($\sigma_w^2(b) = \sigma_w^2 \forall b$), the free energy in (12) simplifies to the result obtained in [24] with one-dimensional argument $E = E(1) = \dots = E(B)$. Replica curves for the isotropic case are shown in Figure 1. The global maximum of $\mathcal{F}(E)$ corresponds to the MMSE whereas BAMP typically achieves the largest MSE associated with a local maximum.

Two-dimensional free energy functions for various rates are depicted in Figure 2. In the top row, the arrows in the MSE plane depict the SE prediction

$$(\text{MSE}^t(1), \text{MSE}^t(2)) \rightarrow (\text{MSE}^{t+1}(1), \text{MSE}^{t+1}(2)).$$

The bottom row shows the free energy function (via gray shading and contour lines). There is a close match between the fixed points of the SE and the stationary points of the free energy function, as well as between the SE arrows and the gradient of the free energy. This match was confirmed in several other numerical experiments.

V. ANISOTROPIC BAMP DYNAMICS

A. Correlated CS

The matrix \mathbf{T} from Algorithm 2 simultaneously decorrelates the signal and the noise. While $\mathbf{T}\Sigma_{\vec{\mathbf{x}}}\mathbf{T}^T = \mathbf{I}$, the transformed noise covariance $\Sigma_{\vec{\mathbf{w}}} = \mathbf{T}\Sigma_{\vec{\mathbf{w}}}\mathbf{T}^T$ depends on $\Sigma_{\vec{\mathbf{x}}}$ and $\Sigma_{\vec{\mathbf{w}}}$ in a nontrivial way unless $\Sigma_{\vec{\mathbf{x}}}$ and $\Sigma_{\vec{\mathbf{w}}}$ commute. In this case, they have identical eigenvectors, i.e., $\Sigma_{\vec{\mathbf{x}}} = \mathbf{Q}\Lambda_{\vec{\mathbf{x}}}\mathbf{Q}^T$ and $\Sigma_{\vec{\mathbf{w}}} = \mathbf{Q}\Lambda_{\vec{\mathbf{w}}}\mathbf{Q}^T$, and we can show

$$\Sigma_{\vec{\mathbf{w}}} = \Lambda_{\vec{\mathbf{w}}}\Lambda_{\vec{\mathbf{x}}}^{-1} = \text{diag} \left(\frac{\lambda_{\vec{\mathbf{w}}}(1)}{\lambda_{\vec{\mathbf{x}}}(1)}, \dots, \frac{\lambda_{\vec{\mathbf{w}}}(B)}{\lambda_{\vec{\mathbf{x}}}(B)} \right).$$

Special cases of this situation occur when (i) either $\Sigma_{\vec{\mathbf{x}}}$ or $\Sigma_{\vec{\mathbf{w}}}$ is a scaled identity matrix and (ii) when both $\Sigma_{\vec{\mathbf{x}}}$ and $\Sigma_{\vec{\mathbf{w}}}$ are diagonal. The per-channel SNRs are then obtained from $\Sigma_{\vec{\mathbf{w}}}$ as $\text{SNR}(b) = \epsilon\lambda_{\vec{\mathbf{x}}}(b)/\lambda_{\vec{\mathbf{w}}}(b)$. While this result does not hold when $\Sigma_{\vec{\mathbf{x}}}$ and $\Sigma_{\vec{\mathbf{w}}}$ do not commute, it is possible to derive the bounds

$$\epsilon \frac{\min_k \{\lambda_{\vec{\mathbf{x}}}(k)\}}{\max_k \{\lambda_{\vec{\mathbf{w}}}(k)\}} \leq \text{SNR}(b) \leq \epsilon \frac{\max_k \{\lambda_{\vec{\mathbf{x}}}(k)\}}{\min_k \{\lambda_{\vec{\mathbf{w}}}(k)\}}.$$

If a subset $\mathbf{x}(b_1), \dots, \mathbf{x}(b_K)$ of the B signal vectors is fully correlated, then $K - 1$ of the SNRs equal 0. Thus, the model is equivalent to one with $B - K + 1$ (instead of B) measurements, but with different SNRs. The free energy function leads to the same conclusion: when taking the limits $\sigma_w^2(b_1) = \dots = \sigma_w^2(b_{K-1}) \rightarrow \infty$ in the B -dimensional free energy function (12), it can be seen that $\mathcal{F}(\vec{\mathbf{E}})$ is independent of $E(b_1), \dots, E(b_{K-1})$. Therefore, the curvature of $\mathcal{F}(\vec{\mathbf{E}})$ and hence the location of its stationary points do not depend on those arguments, such that the B -dimensional free energy function effectively collapses into a $B - K + 1$ -dimensional function.

B. MMSE Gap

In the CS regime of small ϵ , the MMSE estimate $\hat{\mathbf{x}}$ for a single measurement features a phase transition characterized by an abrupt change of the MSE at a certain rate R_{PT} : for rates less than R_{PT} , the MSE tends to be large, whereas for rates larger than R_{PT} the MSE tends to be small. This phenomenon can be seen in Figure 1: for rates below $R \approx 0.16$, the free energy has a single maximum at an MSE of about -12 dB whereas for rates larger than $R \approx 0.17$ a second local maximum at MSEs less than about -37 dB appears.

A similarly abrupt phase transition does not occur when the number of measurements B is large. Figure 3 shows the

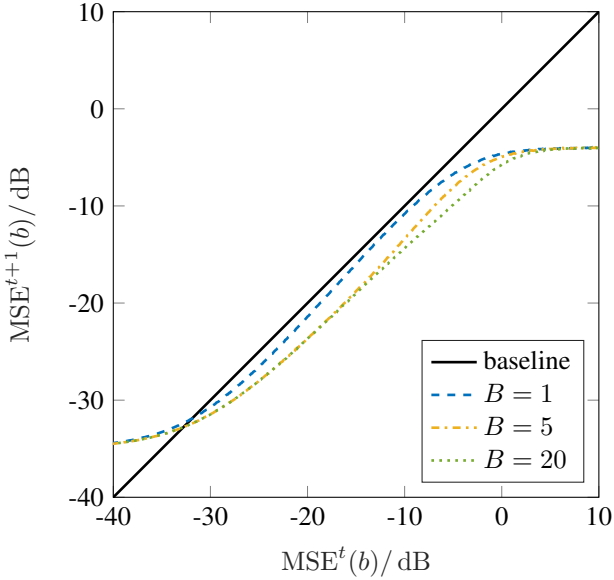


Figure 3: Noisy SE curves for different number of jointly sparse BG signals ($\epsilon = 0.1$, $\Sigma_{\bar{x}} = \mathbf{I}_B$, $\Sigma_{\bar{w}} = -35 \text{ dB } \mathbf{I}_B$, $R = 0.25$).

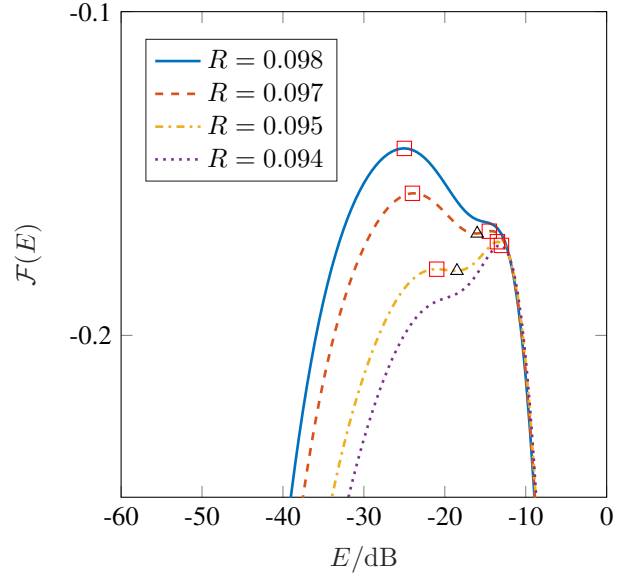


Figure 4: One-dimensional free energy function for $B = 10$ jointly sparse BG vectors at rates around the phase transition rate ($\Sigma_{\bar{w}} = -35 \text{ dB } \mathbf{I}_B$).

(empirical) SE curves for various B with $\epsilon = 0.1$ and $\Sigma_{\bar{x}} = \mathbf{I}_B$ (for BG signals and $\Sigma_{\bar{x}} = \mathbf{I}_B$ the SE is characterized by a single curve since the effective noise covariance is a scaled identity matrix). Observe that the “bump” in the SE curve for small B and large MSE, which corresponds to the first fixed point, flattens out with increasing B ; this suggests that for large B the MSE changes smoothly with increasing rate R . The same conclusion can be obtained by investigating the behavior

of the free energy functions. BAMP typically achieves the largest MSE which corresponds to a local maximum in the free energy, whereas the MSE at the global maximum of the free energy is the MMSE. As pointed out in [24], whenever the free energy function has a second local maximum (not the global maximum) which occurs at a larger MSE than the global maximum, BAMP is not Bayesian-optimal (i.e., does not reach the MMSE).

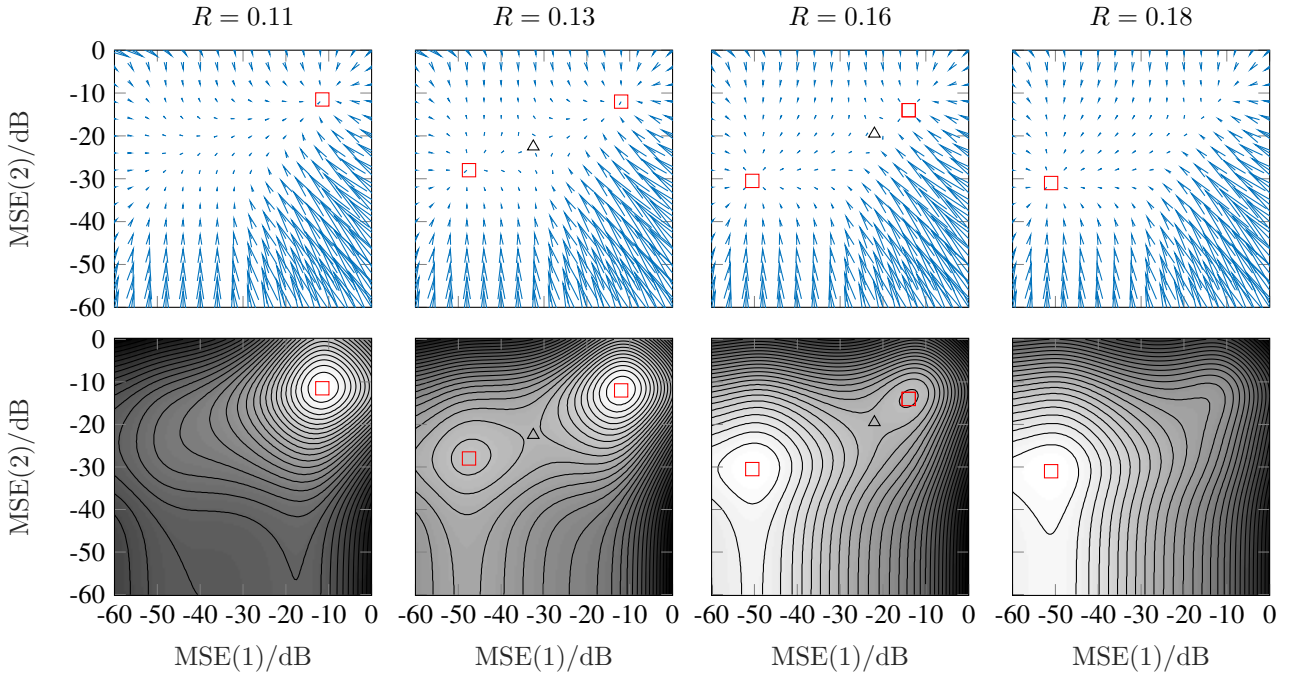


Figure 2: SE (top) and free energy (bottom) for $B = 2$, $\epsilon = 0.1$, $\Sigma_{\bar{x}} = \mathbf{I}_2$, $\sigma_{\bar{w}}^2(1) = -45 \text{ dB}$, and $\sigma_{\bar{w}}^2(2) = -25 \text{ dB}$. Red squares indicate stable fixed points and local maxima whereas black triangles indicate unstable fixed points and saddle points.

In Figure 1, the corresponding rate region is approximately $0.19 < R < 0.21$; for $B = 2$ (cf. Figure 2) two local maxima occur at $R = 0.16$; and for $B = 10$ (and isotropic noise) at $R = 0.097$ (see Figure 3). Thus, the rate region in which there are two local maxima in the free energy shrinks with increasing B and eventually disappears; at the same time, the abrupt transition from high MSE to low MSE becomes softer. We conclude that, as B increases the rate region where BAMP is not Bayesian-optimal shrinks, and, for a sufficiently large B , BAMP is Bayesian-optimal in the complete rate region, i.e., it is the MMSE estimator.

We emphasize that our analysis is asymptotic in the measurement matrix dimensions and the sparsity ($N, M, \epsilon N \rightarrow \infty$), the number of jointly sparse vectors B is non-asymptotic and grows with $\mathcal{O}(1)$. This is in contrast to existing work [35], [36], where results on the phase transition were derived for the asymptotic case where $B \rightarrow \infty$ as $N \rightarrow \infty$.

In the previous examples, we mostly considered the isotropic case ($\sigma_w^2(b) = \sigma_w^2 \forall b$), where the key parameter determining the gap between MMSE and BAMP performance is the effective number of jointly sparse vectors B . The anisotropic free energy formula (12), however, opens up the possibility for more detailed investigations with different sets of parameters $\sigma_w^2(1), \dots, \sigma_w^2(B)$ to shed light on the performance regions and dynamics of BAMP. The questions arises whether for a given sparsity ϵ and measurement rate R there is a diversity function $\theta_{\epsilon,R}(\sigma_w^2(1), \dots, \sigma_w^2(B))$ that describes the effective number of jointly sparse measurements based on the individual SNRs. More specifically, we expect such a diversity function to combine the SNRs such that, for a certain threshold B_0 , the global maximum of the free energy equals the BAMP fixed point for $\theta_{\epsilon,R} \geq B_0$ while for $\theta_{\epsilon,R} < B_0$ the free energy has local maxima to the right of the global maximum, which then is no longer the BAMP fixed point. Upon inspection of Figure 1, we further surmise that the BAMP dynamics exhibit a one-dimensional attracting manifold in the B -dimensional state space/free energy. This raises the question of whether the B -dimensional SE dynamics can be compressed into a one-dimensional evolution.

VI. CONCLUSIONS

We reviewed the multivariate BAMP algorithm for MMV/DCS CS recovery and its associated multivariate SE. We established that for arbitrary MMV measurement models there is an equivalent model in which signal and noise are both decorrelated. For the widely employed multivariate BG signal prior, we proved that uncorrelatedness is preserved during the BAMP and SE iterations; thus, the complexity of BAMP for BG signals scales only linearly with the number of jointly sparse vectors. The free energy formula for the jointly sparse BG CS channel with B degrees of freedom has been derived and juxtaposed with the multivariate SE. Our results allowed us to assess the impact of signal correlation and of the number of jointly sparse vectors on the phase transition phenomenon and the optimality rate region of BAMP.

APPENDIX

A. Equivariance of MMV VBAMP and its SE

Consider Algorithm 1 with the transformed variables $\Sigma_{\tilde{\mathbf{x}}}$, $\mathbf{T}\tilde{\mathbf{x}}_n^t$, $\mathbf{T}\tilde{\mathbf{r}}_m^t$, $\mathbf{T}\tilde{\mathbf{u}}_n^t$, $\Sigma_{\tilde{\mathbf{v}}}^t$. Lines 5 and 6 are trivially equivariant. The equivariance of line 7 follows from the invariance property of MMSE estimators to affine transformations [37, Ch. 11.4]. In the residual term (line 8), the equivariance of $\tilde{\mathbf{y}}_m - (\mathbf{A}(1)\tilde{\mathbf{x}}(1)^t, \dots, \mathbf{A}(B)\tilde{\mathbf{x}}(B)^t)_m$ is trivial. It remains to show that the Onsager term is equivariant. Thus, we write the transformed Onsager term as

$$\begin{aligned} & \frac{1}{M} \sum_{n=1}^N F'(\mathbf{T}\tilde{\mathbf{u}}_n; \mathbf{T}\Sigma_{\tilde{\mathbf{v}}}\mathbf{T}^T) \mathbf{T}\tilde{\mathbf{r}}_m \\ & \stackrel{\{1\}}{=} \frac{1}{M} \sum_{n=1}^N \text{Cov}\{\tilde{\mathbf{x}} \mid \mathbf{T}\tilde{\mathbf{u}}_n; \mathbf{T}\Sigma_{\tilde{\mathbf{v}}}\mathbf{T}^T\} (\mathbf{T}\Sigma_{\tilde{\mathbf{v}}}\mathbf{T}^T)^{-1} \mathbf{T}\tilde{\mathbf{r}}_m \\ & = \frac{1}{M} \sum_{n=1}^N \text{E}\{\langle \tilde{\mathbf{x}} - \text{E}\{\tilde{\mathbf{x}}\} \mid \mathbf{T}\tilde{\mathbf{u}}_n; \mathbf{T}\Sigma_{\tilde{\mathbf{v}}}\mathbf{T}^T \rangle \mathbf{T}^{-T} \Sigma_{\tilde{\mathbf{v}}}^{-1} \tilde{\mathbf{r}}_m\} \\ & = \frac{1}{M} \sum_{n=1}^N \mathbf{T} \text{E}\{\langle \tilde{\mathbf{x}} - \text{E}\{\tilde{\mathbf{x}}\} \mid \tilde{\mathbf{u}}_n; \Sigma_{\tilde{\mathbf{v}}}\rangle \mathbf{T}^T \mathbf{T}^{-T} \Sigma_{\tilde{\mathbf{v}}}^{-1} \tilde{\mathbf{r}}_m\} \\ & \stackrel{\{2\}}{=} \mathbf{T} \frac{1}{M} \sum_{n=1}^N \text{Cov}\{\tilde{\mathbf{x}} \mid \tilde{\mathbf{u}}_n; \Sigma_{\tilde{\mathbf{v}}}\} \Sigma_{\tilde{\mathbf{v}}}^{-1} \tilde{\mathbf{r}}_m \\ & = \mathbf{T} \frac{1}{M} \sum_{n=1}^N F'(\tilde{\mathbf{u}}_n; \Sigma_{\tilde{\mathbf{v}}}) \tilde{\mathbf{r}}_m, \end{aligned}$$

where $\{1\}$ and $\{2\}$ follow from Lemma 2 in Appendix D. The equivariance of SE follows by similar arguments using elementary probability theory and the invariance property of MMSE estimators to affine transformations [37, Ch. 11.4].

B. Diagonality of SE with BG Prior

We show that MMV SE (6) preserves diagonality for the BG prior. In particular, we prove that if $\Sigma_{\tilde{\mathbf{v}}}^t$, $\Sigma_{\tilde{\mathbf{w}}}$ and $\Sigma_{\tilde{\mathbf{x}}}$ are diagonal, then

$$\Sigma_{\tilde{\mathbf{v}}}^{t+1} = \Sigma_{\tilde{\mathbf{w}}} + \frac{1}{R} \underbrace{\text{E}_{\tilde{\mathbf{x}}, \tilde{\mathbf{v}}}\left\{ \langle F(\tilde{\mathbf{x}} + \tilde{\mathbf{v}}^t; \Sigma_{\tilde{\mathbf{v}}}^t) - \tilde{\mathbf{x}} \rangle \right\}}_{\mathbf{C}}$$

is also diagonal. It suffices to establish that \mathbf{C} is diagonal. Inserting the BG prior (2) and its estimator (4) and writing out the integrals for $(\mathbf{C})_{i,j}$ ($i, j = 1, \dots, B$), it is seen that for $i \neq j$ the integrands have odd symmetry w.r.t. a separable set of their arguments and thus integrate to 0. It follows that $(\mathbf{C})_{i,j} = 0$ for $i \neq j$ and that $\Sigma_{\tilde{\mathbf{v}}}^{t+1}$ is diagonal.

C. Replica Analysis

Following the analysis in [24], we derive an analytical performance prediction for the BAMP algorithm for MMV and DCS problems. We consider the measurement model (1) and the signal prior (2) with $\Sigma_{\tilde{\mathbf{x}}} = \mathbf{I}$ and $\tilde{\mathbf{w}}_m \sim \mathcal{N}(\mathbf{0}, \Sigma_{\tilde{\mathbf{w}}})$, where $\Sigma_{\tilde{\mathbf{w}}} = \text{diag}(\sigma_w^2(1), \dots, \sigma_w^2(B))$ is a diagonal matrix with the noise variances $\sigma_w^2(b)$. The special case $\Sigma_{\tilde{\mathbf{w}}} = \sigma_w^2 \mathbf{I}$ was analyzed in [24]. We follow [24] by assuming the rows of $\mathbf{A}(b)$ to have variance $\frac{1}{N}$. The straightforward rescaling to

normalized columns is discussed at the end. For the sake of notational simplicity, the following derivation applies to the MMV scenario, i.e., $\mathbf{A}(1) = \dots = \mathbf{A}(B) = \mathbf{A}$. The generalization to DCS is straightforward (cf. [24]). The posterior pdf of the estimate $\hat{\mathbf{X}} = (\hat{\mathbf{x}}(1), \dots, \hat{\mathbf{x}}(B)) = (\hat{\mathbf{x}}_1, \dots, \hat{\mathbf{x}}_N)^T$ reads

$$f_{\hat{\mathbf{X}}|\mathbf{Y}}(\hat{\mathbf{X}} | \mathbf{Y}) = \frac{1}{Z} \prod_{n=1}^N f_{\hat{\mathbf{x}}_n}(\hat{\mathbf{x}}_n) \prod_{m=1}^M \mathcal{N}((\mathbf{Y} - \mathbf{A}\hat{\mathbf{X}})_m; \mathbf{0}, \Sigma_{\bar{\mathbf{w}}})$$

with $\mathbf{Y} = (\mathbf{y}(1), \dots, \mathbf{y}(B)) = (\vec{\mathbf{y}}_1, \dots, \vec{\mathbf{y}}_M)^T$. Furthermore, Z is the partition function

$$Z = \int_{\mathbb{R}^{NB}} \prod_{m=1}^M \mathcal{N}((\mathbf{Y} - \mathbf{A}\hat{\mathbf{X}})_m; \mathbf{0}, \Sigma_{\bar{\mathbf{w}}}) \prod_{n=1}^N f_{\hat{\mathbf{x}}_n}(\hat{\mathbf{x}}_n) d\hat{\mathbf{x}}_n.$$

Following the argumentation in [24] and the assumptions in [29], [30], [38]–[41], we determine the stationary points of the free energy function, which provide the MSEs in the fixed points of BAMP along with the MMSE for the measurement model (1). The free energy is defined as

$$\mathcal{F} = \lim_{N \rightarrow \infty} \frac{1}{N} \mathbb{E}_{\mathbf{A}, \mathbf{x}, \mathbf{w}} \{\log(Z)\}, \quad (13)$$

but in general is difficult to evaluate. The replica method [29], [30], [38]–[41] introduces k replicas $\hat{\mathbf{X}}^1, \dots, \hat{\mathbf{X}}^k$ of the estimate $\hat{\mathbf{X}}$ and approximates the free energy (13) as

$$\mathcal{F} = \lim_{N \rightarrow \infty} \lim_{k \rightarrow 0} \frac{\mathbb{E}_{\mathbf{A}, \mathbf{x}, \mathbf{w}} \{Z^k\} - 1}{Nk}. \quad (14)$$

The self-averaging property that leads to (13) and the replica trick (14) as well as the replica symmetry assumptions are assumed to be valid, even though their theoretical justification is still an open problem [29], [30], [38]–[41]. In order to evaluate (13), we write

$$\mathbb{E}_{\mathbf{A}, \mathbf{x}, \mathbf{w}} \{Z^k\} = |2\pi \Sigma_{\bar{\mathbf{w}}}|^{-\frac{k}{2}} \mathbb{E}_{\mathbf{X}} \left\{ \int \prod_{m=1}^M \mathbb{X}_m \prod_{n=1}^N \prod_{a=1}^k f_{\bar{\mathbf{x}}_n^a} d\bar{\mathbf{x}}_n^a \right\}, \quad (15)$$

where

$$\mathbb{X}_m = \mathbb{E}_{\mathbf{A}, \mathbf{w}} \left\{ \exp \left(-\frac{1}{2} \|\bar{\mathbf{v}}_m\|^2 \right) \right\}. \quad (16)$$

Here, we used the vector $\bar{\mathbf{v}}_m = \bar{\Sigma}_{\bar{\mathbf{w}}}^{-\frac{1}{2}} \bar{\mathbf{v}}_m$ defined in terms of $\bar{\mathbf{v}}_m = (v_{m,1}^1, \dots, v_{m,1}^k, v_{m,2}^1, \dots, v_{m,2}^k, \dots, v_{m,B}^1, \dots, v_{m,B}^k)^T$, and $\bar{\Sigma}_{\bar{\mathbf{w}}} = \Sigma_{\bar{\mathbf{w}}} \otimes \mathbf{I}_{k \times k}$, where the elements of $\bar{\mathbf{v}}_m$ are in terms of

$$\bar{\mathbf{v}}_m^a = (v_{m,1}^a, \dots, v_{m,B}^a) = (\mathbf{A}(\mathbf{X} - \hat{\mathbf{X}}^a) + \mathbf{W})_m.$$

Using a Gaussian approximation for the pdf of $\bar{\mathbf{v}}_m$,

$$f_{\bar{\mathbf{v}}_m}(\bar{\mathbf{v}}_m) = \mathcal{N}(\bar{\mathbf{v}}_m; \mathbf{0}, \mathbf{G}_m), \quad (17)$$

(16) can be evaluated as

$$\mathbb{X}_m = |\mathbf{I} + \mathbf{G}_m|^{-\frac{1}{2}}. \quad (18)$$

Here, we used the covariance matrix $\mathbf{G}_m = \text{Cov}\{\bar{\mathbf{v}}_m\} = \bar{\Sigma}_{\bar{\mathbf{w}}}^{-\frac{1}{2}} \bar{\mathbf{G}}_m \bar{\Sigma}_{\bar{\mathbf{w}}}^{-\frac{1}{2}}$ with $\mathbf{G}_m = \text{Cov}\{\bar{\mathbf{v}}_m\}$. The matrix $\bar{\mathbf{G}}_m$ is composed of $B \times B$ blocks of size $k \times k$ as follows:

- 1) The main diagonal of $\bar{\mathbf{G}}_m$ consists of entries $g_1(b) = \mathbb{E}_{\mathbf{A}, \mathbf{w}} \{(v_{m,b}^a)^2\}$, which is different in each of the B blocks but identical within a block.
- 2) The remaining entries in the blocks of the main diagonal are $g_2(b) = \mathbb{E}_{\mathbf{A}, \mathbf{w}} \{v_{m,b}^a v_{m,b}^{a'}\}$, which are different in each block but identical within a block.
- 3) The diagonal entries of the off-diagonal blocks are $g_3(b, b') = \mathbb{E}_{\mathbf{A}, \mathbf{w}} \{v_{m,b}^a v_{m,b'}^a\}$.
- 4) The off-diagonal entries of the off-diagonal blocks are $g_4(b, b') = \mathbb{E}_{\mathbf{A}, \mathbf{w}} \{v_{m,b}^a v_{m,b'}^{a'}\}$.

Using the normalization of the measurement matrix \mathbf{A} , the fact that $\bar{\mathbf{x}}_n^a$ follows the same distribution as $\bar{\mathbf{x}}_n$, and the replica symmetry [29], [30], these values turn out to be

$$\begin{aligned} g_1(b) &= \frac{1}{N} \sum_{n=1}^N (x_n(b) - \hat{x}_n^a(b))^2 + 1, \\ g_2(b) &= \frac{1}{N} \sum_{n=1}^N (x_n(b) - \hat{x}_n^a(b))(x_n(b) - \hat{x}_n^{a'}(b)) + 1, \\ g_3(b, b') &= \frac{1}{N} \sum_{n=1}^N (x_n(b) - \hat{x}_n^a(b))(x_n(b') - \hat{x}_n^{a'}(b')), \\ g_4(b, b') &= \frac{1}{N} \sum_{n=1}^N (x_n(b) - \hat{x}_n^a(b))(x_n(b) - \hat{x}_n^{a'}(b')). \end{aligned}$$

By introducing the auxiliary quantities

$$\begin{aligned} m_a(b, b') &= \frac{1}{N} \sum_{n=1}^N \hat{x}_n^a(b) x_n(b'), \\ Q_a(b, b') &= \frac{1}{N} \sum_{n=1}^N \hat{x}_n^a(b) \hat{x}_n^a(b'), \\ q_{aa'}(b, b') &= \frac{1}{N} \sum_{n=1}^N \hat{x}_n^a(b) \hat{x}_n^{a'}(b'), \\ q_0(b, b') &= \frac{1}{N} \sum_{n=1}^N x_n(b) x_n(b'), \end{aligned}$$

the covariance values can be written as

$$\begin{aligned} g_1(b) &= \epsilon - 2m_a(b, b) + Q_a(b, b) + 1, \\ g_2(b) &= \epsilon - m_a(b, b) - m_{a'}(b, b) + q_{aa'}(b, b) + 1, \\ g_3(b, b') &= q_0(b, b') - m_a(b', b) - m_{a'}(b, b) + q_{aa'}(b, b), \\ g_4(b, b') &= q_0(b, b) - m_a(b', b) - m_{a'}(b', b) + q_{aa'}(b', b'). \end{aligned}$$

In the Bayesian setting the distribution of $\bar{\mathbf{x}}_n$ matches the distribution of $\hat{\mathbf{x}}_n$ and that of the replicas $\hat{\mathbf{x}}_n^a$, thus $g_3(b, b') = g_4(b, b') = 0$. Furthermore, due to the replica symmetry [29], [30] $m_a(b, b) = m_{a'}(b, b) = m(b)$, $Q_a(b, b) = Q(b)$, and $q_{aa'}(b, b) = q(b)$. It follows that the \mathbf{G}_m is a structured matrix that, due to its block structure, can be expressed in terms of all-ones matrices, identity matrices, and Kronecker products. Its kB eigenvalues can straightforwardly be determined as

$$\alpha_1^b = g_1(b) + (k-1)g_2(b), \quad \alpha_2^b = g_1(b) - g_2(b),$$

where the α_1^b have multiplicity 1 and the α_2^b have multiplicity $k-1$. We can thus express (18) as

$$|\mathbf{I} + \mathbf{G}_m|^{-\frac{1}{2}} = \left[\prod_{b=1}^B \left(1 + k \frac{\epsilon - 2m(b) + q(b) + \sigma_w^2(b)}{\sigma_w^2(b) + Q(b) - q(b)} \right) \prod_{b=1}^B \left(1 + \frac{1}{\sigma_w^2(b)} (Q(b) - q(b)) \right)^{k-1} \right]^{-\frac{1}{2}}.$$

Using the Taylor series approximation

$$\exp\left(-\frac{x}{2}\right) \approx (1+x)^{-\frac{1}{2}},$$

we obtain

$$\lim_{k \rightarrow 0} \mathbb{X}_m = \exp\left(-\frac{k}{2} \sum_{b=1}^B \frac{\epsilon - 2m(b) + q(b) + \sigma_w^2(b)}{\sigma_w^2(b) + Q(b) - q(b)} - \log(Q(b) - q(b) + \sigma_w^2(b)) - \log(\sigma_w^2(b))\right).$$

Following the derivation in [24, App.], (15) can be written as

$$\mathbb{E}_{\mathbf{A}, \mathbf{x}, \mathbf{w}} \{Z^k\} = \int \exp(kN\Phi(m_0, \hat{m}_0, q, \hat{q}, Q, \hat{Q})) dm_0 d\hat{m}_0 dq d\hat{q} dQ d\hat{Q}.$$

Remember that we are only interested in the stationary points of the free energy expression (15). Thus, we set

$$\begin{aligned} \mathcal{F} &= \Phi(\{m(b)^*, \hat{m}(b)^*, q(b)^*, \hat{q}(b)^*, Q(b)^*, \hat{Q}(b)^*\}_{b=1, \dots, B}) \\ &= \frac{1}{2} \sum_{b=1}^B (Q(b)\hat{Q}(b) - 2m(b)\hat{m}(b) + q(b)\hat{q}(b)) - \frac{R}{2} \log(|2\pi\Sigma_{\mathbf{w}}|) \\ &\quad - \frac{R}{2} \sum_{b=1}^B \left(\frac{\epsilon - 2m(b) + q(b) + \sigma_w^2(b)}{Q(b) - q(b) + \sigma_w^2(b)} \right. \\ &\quad \left. + \log(Q(b) - q(b) + \sigma_w^2(b)) - \log(\sigma_w^2(b)) \right) \\ &\quad + \int_{\mathbb{R}^B} f_{\mathbf{x}}(\bar{\mathbf{x}}) \int_{\mathbb{R}^B} \log \int_{\mathbb{R}^B} f_{\hat{\mathbf{x}}}(\hat{\mathbf{x}}) \\ &\quad \prod_{b=1}^B \exp\left(-\frac{1}{2}\hat{q}(b)\hat{x}(b)^2 + \hat{m}(b)\hat{x}(b)x(b) + \sqrt{\hat{m}(b)}\hat{x}(b)h(b)\right) d\hat{\mathbf{x}} \mathcal{D}\bar{\mathbf{h}} d\hat{\mathbf{x}}, \end{aligned} \quad (19)$$

where the superscript $*$ denotes stationary points. The stationary points are obtained by derivation as

$$\begin{aligned} \frac{d\Phi}{dm(b)} = 0 &\Rightarrow \hat{m}(b)^* = \frac{R}{E(b) + \sigma_w^2(b)} = \gamma(b) \\ \frac{d\Phi}{dq(b)} = 0 &\Rightarrow \hat{q}(b)^* = \frac{R}{E(b) + \sigma_w^2(b)} = \gamma(b) \\ \frac{d\Phi}{dQ(b)} = 0 &\Rightarrow \hat{Q}(b)^* = 0, \end{aligned}$$

where we used the substitution $E(b) = Q(b) - q(b)$, and the fact that in the Bayesian setting $q(b)^* = m(b)^*$, and $Q(b)^* = \epsilon$. Substituting back into (19) and using $\bar{\mathbf{E}} = (E(1), \dots, E(B))^T$, we obtain

$$\begin{aligned} \mathcal{F}(\bar{\mathbf{E}}, \Sigma_{\mathbf{w}}) &= \\ &- \frac{R}{2} \sum_{b=1}^B \left(\log(2\pi(\sigma_w^2(b) + E(b))) + \frac{\epsilon + \sigma_w^2(b)}{E(b) + \sigma_w^2(b)} \right) \\ &\quad + \int_{\mathbb{R}^B} f_{\mathbf{x}}(\bar{\mathbf{x}}) \int_{\mathbb{R}^B} \log \left(\int_{\mathbb{R}^B} f_{\hat{\mathbf{x}}}(\hat{\mathbf{x}}) \right. \\ &\quad \left. \prod_{b=1}^B \exp\left(-\frac{1}{2}\gamma(b)\hat{x}(b)^2 + \gamma(b)\hat{x}(b)x(b) + \sqrt{\gamma(b)}\hat{x}(b)h(b)\right) d\hat{\mathbf{x}} \right) \mathcal{D}\bar{\mathbf{h}} d\hat{\mathbf{x}}. \end{aligned}$$

where the second integration is over a standard Gaussian measure, i.e., $\mathcal{D}\mathbf{h} = \prod_{b=1}^B \mathcal{N}(h_b; 0, 1) dh_b = \mathcal{N}(\mathbf{h}; \mathbf{0}, \mathbf{I}) \prod_{b=1}^B dh_b$. Inserting the signal prior (2) results in

$$\begin{aligned} \mathcal{F}(\bar{\mathbf{E}}, \Sigma_{\mathbf{w}}) &= -\frac{R}{2} \sum_{b=1}^B \left(\log(2\pi(\sigma_w^2(b) + E(b))) + \frac{\epsilon + \sigma_w^2(b)}{E(b) + \sigma_w^2(b)} \right) \\ &\quad + (1-\epsilon) \int \log\left((1-\epsilon) + \right. \\ &\quad \left. \epsilon \int \exp\left(-\frac{1}{2}\gamma(b)\hat{x}^2 + \sqrt{\gamma(b)}\hat{x}(b)h(b)\right) \mathcal{D}\mathbf{x} \right) \mathcal{D}\bar{\mathbf{h}} \\ &\quad + \epsilon \int \int \log\left((1-\epsilon) + \right. \\ &\quad \left. \epsilon \int \exp\left(-\frac{1}{2}\gamma(b)\hat{x}(b)^2 + \gamma(b)\hat{x}(b)x(b) + \sqrt{\gamma(b)}\hat{x}(b)h(b)\right) \mathcal{D}\hat{\mathbf{x}} \right) \mathcal{D}\bar{\mathbf{h}} \mathcal{D}\bar{\mathbf{x}}, \end{aligned}$$

with the measure $\mathcal{D}\bar{\mathbf{x}}$ and $\mathcal{D}\hat{\mathbf{x}}$ analogously to the above. Writing out the integration measures and further simplifying leads to

$$\begin{aligned} \mathcal{F}(\bar{\mathbf{E}}, \Sigma_{\mathbf{w}}) &= -\frac{R}{2} \sum_{b=1}^B \left(\log(2\pi(\sigma_w^2(b) + E(b))) + \frac{\epsilon + \sigma_w^2(b)}{E(b) + \sigma_w^2(b)} - \frac{\gamma(b)(1 + \epsilon\gamma(b))}{R(1 + \gamma(b))} \right) \\ &\quad + (1-\epsilon) \int \log\left(\epsilon \prod_{b=1}^B (1 + \gamma(b))^{-\frac{1}{2}} + (1-\epsilon) \exp\left(-\frac{1}{2} \sum_{b=1}^B \gamma(b)h^2(b)\right)\right) \mathcal{D}\bar{\mathbf{h}} \\ &\quad + \epsilon \int \log\left(\epsilon \prod_{b=1}^B (1 + \gamma(b))^{-\frac{1}{2}} + (1-\epsilon) \exp\left(-\frac{1}{2} \sum_{b=1}^B \frac{\gamma(b)}{1 + \gamma(b)} h^2(b)\right)\right) \mathcal{D}\bar{\mathbf{h}}. \end{aligned}$$

In order to arrive at (12) that is valid for measurement matrices with normalized columns we use the equivalence between the measurement models with normalized rows and normalized columns and replace $\sigma_w^2(b)$ with $R\sigma_w^2(b)$:

$$\begin{aligned} \mathbf{y} = \mathbf{A}\mathbf{x} + \mathbf{w} &\Leftrightarrow \frac{1}{\sqrt{R}}\mathbf{y} = \bar{\mathbf{A}}\mathbf{x} + \frac{1}{\sqrt{R}}\mathbf{w} \\ &= \bar{\mathbf{y}} = \bar{\mathbf{A}}\mathbf{x} + \bar{\mathbf{w}} \end{aligned}$$

where $\bar{\mathbf{A}}$ has normalized columns and $\bar{\mathbf{w}}_m \sim \mathcal{N}(0, \frac{\sigma_w^2}{R})$ if $\mathbf{w}_m \sim \mathcal{N}(0, \sigma_w^2)$.

D. Estimator Derivative and Conditional Correlation

Lemma 2: Given a realization \mathbf{x} of a random vector $\mathbf{x} \in \mathbb{R}^N$ with pdf $f_{\mathbf{x}}(\mathbf{x})$ and its noisy observation

$$\mathbf{u} = \mathbf{x} + \mathbf{w}$$

with $\mathbf{w} \sim \mathcal{N}(0, \Sigma_{\mathbf{w}})$ being independent additive Gaussian noise, its MMSE estimator is

$$\hat{\mathbf{x}}(\mathbf{u}) = \mathbb{E}\{\mathbf{x} \mid \mathbf{u} = \mathbf{u}\}.$$

Then, the following relation holds:

$$\text{Cov}\{\mathbf{x} \mid \mathbf{u} = \mathbf{u}\} = \frac{d}{d\mathbf{u}^T} \hat{\mathbf{x}}(\mathbf{u}) \Sigma_{\bar{\mathbf{w}}}.$$

Proof 1: Given the definition of the conditional mean and covariance,

$$\begin{aligned} \mathbb{E}\{\mathbf{x} \mid \mathbf{u}, \Sigma_{\bar{\mathbf{w}}}\} &= \frac{1}{f_{\mathbf{u}}(\mathbf{u})} \int_{\mathbb{R}^N} \mathbf{x} f_{\mathbf{u}|\mathbf{x}}(\mathbf{u} \mid \mathbf{x}) f_{\mathbf{x}}(\mathbf{x}) d\mathbf{x} \\ \text{Cov}\{\mathbf{x} \mid \mathbf{u}, \Sigma_{\bar{\mathbf{w}}}\} &= \frac{1}{f_{\mathbf{u}}(\mathbf{u})} \int_{\mathbb{R}^N} \mathbf{x}\mathbf{x}^T f_{\mathbf{u}|\mathbf{x}}(\mathbf{u} \mid \mathbf{x}) f_{\mathbf{x}}(\mathbf{x}) d\mathbf{x} \\ &\quad - \mathbb{E}\{\mathbf{x} \mid \mathbf{u}\} \mathbb{E}\{\mathbf{x} \mid \mathbf{u}\}^T, \end{aligned}$$

we have

$$\begin{aligned} \frac{d}{d\mathbf{u}} \hat{\mathbf{x}}(\mathbf{u}) \Sigma_{\bar{\mathbf{w}}} &= \frac{1}{f_{\mathbf{u}}(\mathbf{u})} \int_{\mathbb{R}^N} \mathbf{x} f_{\mathbf{x}}(\mathbf{x}) \frac{d}{d\mathbf{u}^T} f_{\mathbf{u}|\mathbf{x}}(\mathbf{u} | \mathbf{x}) d\mathbf{x} \Sigma_{\bar{\mathbf{w}}} \\ &- \int_{\mathbb{R}^N} \frac{1}{f_{\mathbf{u}}(\mathbf{u})} \mathbf{x} f_{\mathbf{u}|\mathbf{x}}(\mathbf{u} | \mathbf{x}) f_{\mathbf{x}}(\mathbf{x}) d\mathbf{x} \frac{1}{f_{\mathbf{u}}(\mathbf{u})} \frac{d}{d\mathbf{u}^T} f_{\mathbf{u}}(\mathbf{u}) \Sigma_{\bar{\mathbf{w}}}. \end{aligned} \quad (20)$$

Since $f_{\mathbf{u}|\mathbf{x}}(\mathbf{u} | \mathbf{x}) = \mathcal{N}(\mathbf{0}, \Sigma_{\bar{\mathbf{w}}})$ [42],

$$\frac{d}{d\mathbf{u}^T} f_{\mathbf{u}|\mathbf{x}}(\mathbf{u} | \mathbf{x}) = f_{\mathbf{u}|\mathbf{x}}(\mathbf{u} | \mathbf{x}) (\mathbf{x} - \mathbf{u})^T \Sigma_{\bar{\mathbf{w}}}^{-1}. \quad (21)$$

Furthermore, the MMSE estimator can also be written as [43], [44]

$$\hat{\mathbf{x}}(\mathbf{u}) = \mathbf{u} + \Sigma_{\bar{\mathbf{w}}} \frac{1}{f_{\mathbf{u}}(\mathbf{u})} \frac{d}{d\mathbf{u}} f_{\mathbf{u}}(\mathbf{u}). \quad (22)$$

Combining (20), (21), and (22) we have

$$\begin{aligned} \frac{d}{d\mathbf{u}} \hat{\mathbf{x}}(\mathbf{u}) \Sigma_{\bar{\mathbf{w}}} &= \frac{1}{f_{\mathbf{u}}(\mathbf{u})} \int_{\mathbb{R}^N} \mathbf{x} f_{\mathbf{u}|\mathbf{x}}(\mathbf{x} | \mathbf{u}) (\mathbf{x} - \mathbf{u})^T f_{\mathbf{x}}(\mathbf{x}) d\mathbf{x} \\ &- (\hat{\mathbf{x}}(\mathbf{u}) - \mathbf{u}) \frac{1}{f_{\mathbf{u}}(\mathbf{u})} \int_{\mathbb{R}^N} \mathbf{x} f_{\mathbf{u}|\mathbf{x}}(\mathbf{u} | \mathbf{x}) f_{\mathbf{x}}(\mathbf{x}) d\mathbf{x} \\ &= \frac{1}{f_{\mathbf{u}}(\mathbf{u})} \int_{\mathbb{R}^N} \mathbf{x} \mathbf{x}^T f_{\mathbf{u}|\mathbf{x}}(\mathbf{u} | \mathbf{x}) f_{\mathbf{x}}(\mathbf{x}) d\mathbf{x} - \hat{\mathbf{x}}(\mathbf{u}) \hat{\mathbf{x}}(\mathbf{u})^T \\ &= \text{Cov} \{ \mathbf{x} | \mathbf{u} \}, \end{aligned}$$

which completes the proof.

REFERENCES

- [1] D. L. Donoho, "Compressed Sensing," *IEEE Transactions on Information Theory*, vol. 52, no. 4, pp. 1289–1306, 2006.
- [2] E. J. Candés, J. K. Romberg, and T. Tao, "Stable signal recovery from incomplete and inaccurate measurements," *Communications on Pure and Applied Mathematics*, vol. 59, no. 8, pp. 1207–1223, 2006.
- [3] S. Cotter, B. Rao, K. Engan, and K. Kreutz-Delgado, "Sparse solutions to linear inverse problems with multiple measurement vectors," *IEEE Transactions on Signal Processing*, vol. 53, pp. 2477–2488, Jul. 2005.
- [4] M. F. Duarte, S. Sarvotham, M. B. Wakin, D. Baron, and R. G. Baraniuk, "Joint sparsity models for distributed compressed sensing," in *Proceedings of the Workshop on Signal Processing with Adaptive Sparse Structured Representations*, IEEE, 2005.
- [5] D. Liang, L. Ying, and F. Liang, "Parallel MRI Acceleration Using M-FOCUSS," in *3rd International Conference on Bioinformatics and Biomedical Engineering (ICBBE)*, pp. 1–4, IEEE, 2009.
- [6] T. Wimalajeewa and P. K. Varshney, "OMP based joint sparsity pattern recovery under communication constraints," *IEEE Transactions on Signal Processing*, vol. 62, no. 19, pp. 5059–5072, 2014.
- [7] M. Mayer, G. Hannak, and N. Goertz, "Exploiting Joint Sparsity in Compressed Sensing-based RFID," *EURASIP Journal on Embedded Systems*, vol. 2016, no. 1, pp. 1–15, 2016.
- [8] G. Tzagarakis, D. Miliotis, and P. Tsak, "Multiple-measurement Bayesian compressed sensing using GSM priors for DOA estimation," in *IEEE International Conference on Acoustics Speech and Signal Processing (ICASSP)*, pp. 2610–2613, 2010.
- [9] J. A. Tropp, A. C. Gilbert, and M. J. Strauss, "Algorithms for simultaneous sparse approximation. Part I: Greedy pursuit," *Signal Processing*, vol. 86, no. 3, pp. 572–588, 2006.
- [10] J. A. Tropp, "Algorithms for simultaneous sparse approximation. Part II: Convex relaxation," *Signal Processing*, vol. 86, no. 3, pp. 589–602, 2006.
- [11] D. P. Wipf and B. D. Rao, "An empirical Bayesian strategy for solving the simultaneous sparse approximation problem," *IEEE Transactions on Signal Processing*, vol. 55, no. 7, pp. 3704–3716, 2007.
- [12] M. E. Davies and Y. C. Eldar, "Rank Awareness in Joint Sparse Recovery," *IEEE Transactions on Information Theory*, vol. 58, no. 2, pp. 1135–1146, 2012.
- [13] P. Schniter, "Turbo reconstruction of structured sparse signals," in *2010 44th Annual Conference on Information Sciences and Systems (CISS)*, pp. 1–6, Mar. 2010.
- [14] J. Ziniel and P. Schniter, "Efficient high-dimensional inference in the multiple measurement vector problem," *IEEE Transactions on Signal Processing*, vol. 61, pp. 340–354, Jan. 2013.
- [15] M. Mayer and N. Goertz, "Bayesian Optimal Approximate Message Passing to Recover Structured Sparse Signals," *ArXiv e-prints*, Aug. 2015.
- [16] X. Zhao and W. Dai, "On joint recovery of sparse signals with common supports," in *International Symposium on Information Theory (ISIT)*, pp. 541–545, IEEE, 2015.
- [17] Y. Lu and W. Dai, "Independent versus repeated measurements: A performance quantification via state evolution," in *International Conference on Acoustics, Speech and Signal Processing (ICASSP)*, pp. 4653–4657, IEEE, 2016.
- [18] J. Kim, W. Chang, B. Jung, D. Baron, and J. C. Ye, "Belief propagation for joint sparse recovery," *arXiv preprint arXiv:1102.3289*, 2011.
- [19] D. L. Donoho, A. Maleki, and A. Montanari, "Message-passing algorithms for compressed sensing," *Proceedings of the National Academy of Sciences*, vol. 106, no. 45, pp. 18914–18919, 2009.
- [20] D. Donoho, A. Maleki, and A. Montanari, "Message passing algorithms for compressed sensing: I. motivation and construction," in *2010 IEEE Information Theory Workshop on Information Theory (ITW 2010, Cairo)*, pp. 1–5, Jan. 2010.
- [21] D. Donoho, A. Maleki, and A. Montanari, "Message passing algorithms for compressed sensing: II. analysis and validation," in *2010 IEEE Information Theory Workshop on Information Theory (ITW 2010, Cairo)*, pp. 1–5, Jan. 2010.
- [22] A. Maleki, "Approximate message passing algorithms for compressed sensing." <http://www.ece.rice.edu/~mam15/thesis.pdf>, PhD Thesis, Department of Electrical Engineering, Stanford University, 2011.
- [23] A. Montanari, "Graphical Models Concepts in Compressed Sensing," *Compressed Sensing: Theory and Applications*, pp. 394–438, 2012.
- [24] J. Zhu, D. Baron, and F. Krzakala, "Performance limits for noisy multi-measurement vector problems," *IEEE Transactions on Signal Processing*, 2016.
- [25] M. Bayati and A. Montanari, "The dynamics of message passing on dense graphs, with applications to compressed sensing," *IEEE Transactions on Information Theory*, vol. 57, pp. 764–785, Feb. 2011.
- [26] S. Foucart and H. Rauhut, *A mathematical introduction to compressive sensing*, vol. 1. Birkhäuser Basel, 2013.
- [27] R. A. Horn and C. R. Johnson, *Matrix analysis*. Cambridge university press, 2012.
- [28] J. Vila and P. Schniter, "Expectation-maximization gaussian-mixture approximate message passing," *IEEE Transactions on Signal Processing*, vol. 61, pp. 4658–4672, Oct. 2013.
- [29] F. Krzakala, M. Mézard, F. Sausset, Y. Sun, and L. Zdeborová, "Probabilistic reconstruction in compressed sensing: algorithms, phase diagrams, and threshold achieving matrices," *Journal of Statistical Mechanics: Theory and Experiment*, vol. 2012, no. 08, p. P08009, 2012.
- [30] F. Krzakala, M. Mézard, F. Sausset, Y. Sun, and L. Zdeborová, "Statistical-physics-based reconstruction in compressed sensing," *Physical Review X*, vol. 2, no. 2, p. 021005, 2012.
- [31] G. Reeves and H. D. Pfister, "The replica-symmetric prediction for compressed sensing with gaussian matrices is exact," in *2016 IEEE International Symposium on Information Theory (ISIT)*, pp. 665–669, IEEE, 2016.
- [32] T. Heskes, "Stable fixed points of loopy belief propagation are minima of the Bethe free energy," *Advances in neural information processing systems*, vol. 15, pp. 359–366, 2003.
- [33] J. S. Yedidia, W. T. Freeman, and Y. Weiss, "Constructing free-energy approximations and generalized belief propagation algorithms," *IEEE Transactions on Information Theory*, vol. 51, no. 7, pp. 2282–2312, 2005.
- [34] J. S. Yedidia, W. T. Freeman, and Y. Weiss, "Bethe free energy, Kikuchi approximations, and belief propagation algorithms," *Advances in neural information processing systems*, vol. 13, 2001.
- [35] J. D. Blanchard and M. E. Davies, "Recovery guarantees for rank aware pursuits," *IEEE Signal Processing Letters*, vol. 19, no. 7, pp. 427–430, 2012.
- [36] J. M. Kim, O. K. Lee, and J. C. Ye, "Compressive MUSIC: Revisiting the link between compressive sensing and array signal processing," *IEEE Transactions on Information Theory*, vol. 58, no. 1, pp. 278–301, 2012.
- [37] S. M. Kay, *Fundamentals of statistical signal processing, volume I: estimation theory*. Prentice Hall, 1993.
- [38] T. Tanaka, "A statistical-mechanics approach to large-system analysis of CDMA multiuser detectors," *IEEE Transactions on Information Theory*, vol. 48, no. 11, pp. 2888–2910, 2002.
- [39] D. Guo and S. Verdú, "Randomly spread CDMA: Asymptotics via statistical physics," *IEEE Transactions on Information Theory*, vol. 51, no. 6, pp. 1983–2010, 2005.

- [40] M. Mezard and A. Montanari, *Information, Physics, and Computation*. Oxford University Press, 2009.
- [41] J. Barbier and F. Krzakala, "Approximate message-passing decoder and capacity-achieving sparse superposition codes," *arXiv preprint arXiv:1503.08040*, 2015.
- [42] K. B. Petersen and M. S. Pedersen, "The matrix cookbook," *Technical University of Denmark*, vol. 7, p. 15, 2008.
- [43] M. Raphan and E. P. Simoncelli, "Empirical Bayes least squares estimation without an explicit prior," *NYU Courant Inst. Tech. Report*, 2007.
- [44] M. Raphan and E. P. Simoncelli, "Least squares estimation without priors or supervision," *Neural computation*, vol. 23, no. 2, pp. 374–420, 2011.